

Received 8 April 2023, accepted 8 May 2023, date of publication 19 May 2023, date of current version 30 May 2023.

Digital Object Identifier 10.1109/ACCESS.2023.3278054

## RESEARCH ARTICLE

# Image-Based Partial Discharge Identification in High Voltage Cables Using Hybrid Deep Network

OBABD ALDOSARI<sup>1</sup>, (Member, IEEE), MOHAMMED A. ALDOWSARI<sup>2</sup>, (Member, IEEE),  
SALEM BATIYAH<sup>3</sup>, (Member, IEEE), AND N. KANAGARAJ<sup>1</sup>, (Member, IEEE)

<sup>1</sup>Department of Electrical Engineering, College of Engineering, Prince Sattam Bin Abdulaziz University, Wadi Ad-Dawasir 11991, Saudi Arabia

<sup>2</sup>Department of Electrical Engineering, College of Engineering, King Khaled University, Abha 62529, Saudi Arabia

<sup>3</sup>Department of Electrical and Electronics Engineering Technology, Yanbu Industrial College, Yanbu Industrial, Al Madinah Al Munawwarah 46452, Saudi Arabia

Corresponding author: Obaid Aldosari (om.aldosari@psau.edu.sa)

This work was supported by the Deputyship for Research & Innovation, Ministry of Education, Saudi Arabia, under Project IF-PSAU-2021/01/18739.

**ABSTRACT** Deep learning and digital image technologies have combined to create a potentially effective tool for identifying partial discharge (PD) patterns precisely. However, it is necessary to investigate which algorithm guarantees the best performance. The more common tools are restricted by a lack of training data and an advanced model in itself. Therefore, the main goal of this paper is to develop an efficient hybrid network comprising two deep networks, long short-term memory (LSTM), and convolutional neural network (CNN), for identifying the form of PD. A total of  $8186 \times 25$  (non-PD  $\times$  PD) images were applied to assess the proposed methods. The size of the PD type was increased to 3675 images using data augmentation techniques. The results indicated that the integration of CNN and LSTM networks can provide a more robust implementation for PD detection. The integrated CNN-LSTM deep network based on data augmentation outperformed features derived from a single deep network. The recall, F-measure, and classification precision have 99.9% as a validation accuracy with a 99.8% intersection over union and a loss of 0.004.

**INDEX TERMS** Partial discharge, RGB, gray, data augmentation, LSTM, CNN.

## I. INTRODUCTION

Monitoring, partial discharges (PD) are necessary for determining the condition of cable insulation and boosting the dependability of power distribution and transmission systems [1], [2]. There have been more reports in recent years regarding industrial applications that employ PD for offline or online condition monitoring and issue diagnostics [3]. However, recognizing the various sorts of defects using PD data has proven to be a formidable obstacle, limiting the widespread implementation of PD-based condition monitoring in the industry. It is extremely challenging to differentiate PD signals caused by insulation flaws due to their similarities in PD pattern structure [4].

Various pattern recognition techniques have been employed to recognize PD patterns in an effort to overcome

The associate editor coordinating the review of this manuscript and approving it for publication was Nazar Zaki<sup>1</sup>.

the difficulty of distinguishing between defect types. These approaches involve decision tree (DT), rough set (RS) theory, back propagation neural network (BPNN), and support vector machine (SVM) [5], [6]. Because of their outstanding and reliable pattern recognition capabilities, SVM and BPNN have been the most commonly used approaches [6]. Reference [7] employed wavelet transforms in conjunction with SVM to distinguish PD signals from a variety of sources. Reference [5] implemented particle swarm optimization for tuning SVM parameters to find PD signals in gas-insulated switchgear (GIS). Reference [6] integrated two kinds of BPNN with the input considerations of time-resolved PD form and phase-resolved PD form to develop the pattern identification accuracy of many kinds of PD signals from GIS.

Conventional methods for machine learning, for instance, BPNN and SVM, have been identified to have bottlenecks in their development, limiting future increases in their pattern identification accuracy. In the last decay, deep learning (DL)

has been more significant in the improvement of artificial intelligence and pattern detection systems [8]. Deep neural networks with numerous nonlinear layers are used in DL approaches. It is capable of capturing high-dimensional nonlinearity and complicated correlation that typical shallow neural network topologies cannot learn [9]. Deep neural networks with many nonlinear layers are used in DL techniques. These are able to learn high-dimensional non-linearity and complex correlation, which are not captured by more conventional, shallow neural network architectures.

CNN-based deep learning algorithms are becoming important in the power sector and have been effectively implemented in various disciplines, including voice recognition and image identification [8], [10]. In contrast with other DL approaches, CNN's complexity and difficulty in training are considerably decreased by the sharing and local connection parameters, which also lower the risk of over-fitting [9]. CNN makes it very simple to build a network with a deep architecture [9]. CNN is a deep feedforward neural network, which allows it to efficiently extract spatial properties of signals but it is not for processing time series data. Long-short-term memory (LSTM) networks can analyze time series data, establish the appropriate lag time, and predict time series data extremely successfully [11].

The superiority of DL algorithms in PD identification relies on three primary factors: data augmentation, selecting the optimal feature for an image in color space, and combining different training deep networks. Fundamentally, several preliminary studies have applied data augmentation that can influence the PD detection model while training the model. Data augmentation has been established as a valuable approach to the process of image classification. This technique has demonstrated its effectiveness in mitigating over-fitting issues commonly encountered in models. By repeating several modifications, such as turning or spinning the picture, the advanced technique of "data augmentation" can expand the amount of a dataset [12]. The PD form discovery precision is enhanced by 0.99% when tested with SVM and Random Forest using the Variable Noise Superposition data augmentation approach [13].

The best feature of a color space image is a different element that could be decisive to our investigation. There are many researches work that applied digital images to diagnose PD [13], [14]. These images may be converted into CMYK (cyan-magenta-yellow-black), RGB (red-green-blue), HSV (hue-saturation-value), and grayscale color spaces [15], then utilized as color characteristics. In this work, incorporating different DL models is an important component to increase the quality and resilience of the PD detection model. The CNN-LSTM has better pattern detection performance compared with the CNN network and LSTM network for the defect of metal protrusion, surface discharge, and oil paper void [16]. Reference [11] indicated that CNN-LSTM has the greatest pattern detection rate for diagnosing GIS PD, with an average of 97.9%, and its total precision is greater than other standard analytic approaches.

Despite the fact that these strategies are frequently utilized for PD detection and are effective in PD identification, the high-performance algorithm could be investigated with an accuracy rate of 100%. Furthermore, few research has compared the efficiency and precision of various deep networks, especially LSTM, CNN, and CNN-LSTM with data augmentation, to discover PD patterns in high-voltage cables. Therefore, the aim of this paper is to (i) present how a robust detection of PD-based digital pictures implemented using a hybrid deep network as it is an indicator for making decisions about high voltage cables isolation status (ii) apply LSTM and CNN model to support unlike types of color space images, (iii) combine characteristics acquired from several deep networks which improve the behavior of the produced model, and (iv) investigate the high-quality elements of the hybrid deep network.

The remainder of this paper is organized as follows. The data collection and preparation are explained in Section II. Section III describes the proposed method including the performance analysis. Section IV discuss the results and the evaluation of the proposed method. The conclusion is remarked in Section V.

## II. DATA COLLECTION AND PREPARATION

### A. DATASET DESCRIPTION

On Kaggle, one of the largest data science collaboration platforms in the world, the Technical University of Ostrava (VSB) published the ENET (Centre in Czech Republic) data set in 2018. There are 8711 labeled voltage signals in total from four different locations in the data collection. These areas are intended for use in practical settings (forested and difficult-to-access terrain). Each signal has an 800,000-data-point 50-Hz voltage waveform that is pre-marked as PD (525) or non-PD (8186). The Hadoop distributed file system storage format is used because the data collection is so large. Examples of PD and non-PD signals are presented in Fig. 1. As can be seen, the oscillation of the non-PD signals is fairly stable, whereas that of the PD signals is significantly increased.

### B. SPLIT DATASET AND SOFTWARE

A total of  $8186 \times 25$  images (non-PD  $\times$  PD) were split into training and testing with corresponding sizes of  $6550 \times 420$  and  $1636 \times 105$ , respectively. In addition, the augmented version of  $8186 \times 3675$  images was applied for data analysis. The dataset was divided into 80% and 20% samples for training, and validation, respectively. Analysis methods were carried out in Python 3.7.10 with the assistance of deep learning modules. The data analysis and model development were completed using the Kaggle platform which gives free access to NVidia K80 GPUs embedded system. This benchmark indicates that adding a graphic processing unit (GPU) to our kernel leads to a 12.5X speedup during deep learning model training. The simulation of this case study was conducted using a PC with a Core i7-3630QM CPU, 2.4GHz, and

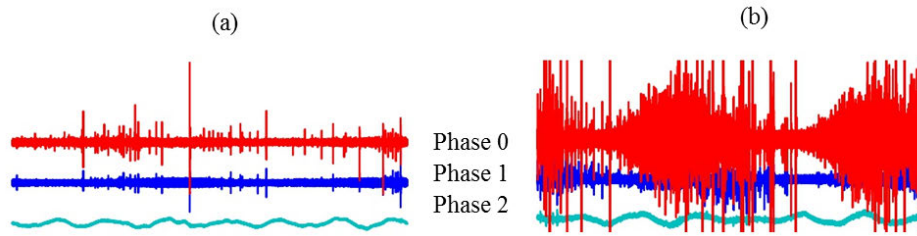


FIGURE 1. ENET dataset signal examples: (a) normal type (non-PD) and (b) PD type.

8.0 GB of RAM. The CCN and LSTM units which were obtained from the TensorFlow library 2.6.2 version to be used for the regression task.

### C. IMAGE PREPROCESSING

This system involves steps like data augmentation to raise the dimension of the trained dataset and reform to normalize the features. First, data augmentation is a significant step for improving the process of learning and enabling the network to recognize objects for photographs taken under various environmental conditions. The reason for using the augmentation process in this study is to enhance confidence in the classification process. As exhibited in Fig. 2, image-based data augmentation dealings, such as a shear range of 0.2, a zoom range of 0.2, a rotation range of 90, a horizontal flip, a width shift range of 0.01, and a height shift range of 0.01, have been implemented. Second, normalization is changed across specific elements to consider the magnitude differences across various features ( $f$ ). By subtracting the minimal image data from the maximum feature value and dividing the variation between them, the feature normalization  $f_{norm}$  can be determined as the following:

$$f_{norm} = \frac{f - f_{min}}{f_{max} - f_{min}} \quad (1)$$

where  $f_{min}$  and  $f_{max}$  are the minimum and maximum feature values of the image data, respectively.

## III. PROPOSED METHOD

### A. DEEP LEARNING MODELS

#### 1) CONVOLUTIONAL NEURAL NETWORK (CNN)

The Convolutional Neural Network is usually employed for two-dimensional input data, with a feed-forward deep learning structure which is the product of the number of data channels ( $n$ ), width ( $w$ ), and height ( $h$ ). The CNN algorithm is made of input layers, hidden layers, and output layers. The main data of the network is considered to be the input layers. The model was provided with grayscale and RGB color space images as its inputs. The grayscale images have a corresponding value of 1 band ( $n = 1$ ), while the RGB images have a corresponding value of 3 bands.

Convolutional layers and pooling are an example of the basic structure of the hidden layers. Based on the number of classes, the output layers are generated by utilizing fully connected layers. The CNN design consists of completely

linked layers whereas the input matrix is smoothed and directed to convert the output toward a single expected value. Fig. 3 presents the proposed deep network architecture of CNN with RGB images. Convolutional layers in the proposed framework function as aspects are taken out from tiny slices of complete data using kernels or filters. The output layer  $O_i^l$  that was used to estimate the descriptive features can be calculated as follow:

$$O_i^l = B_i^l + \sum_i^{m_1(l-1)} K_{i,j}^{(l)} \times O_j^{(l-1)} \quad (2)$$

where  $B_i^l$ ,  $K_{(i,j)}^l$ , and  $m_1^l$  are the bias matrix, the filter linking, and the feature maps, respectively.

For each layer, a collection of convolutional kernels (filters) are used to perform a variety of changes. This filter is manipulated to the input slice whereas the non-linear operational unit is observing the filter's output which simplifies the training process to abstract the embedded nonlinearity of the space feature [17]. Non-linear processing facilitates learning semantic differences throughout the entire image by providing a variety of activation patterns that correlate to a range of responses. Then, the pooling layers that use max-pooling to collect the highly important characteristics minimize the output dimension. The over-fitting issue is resolved by using  $2 \times 2$  max-pooling layers that have been primarily applied to the derived matrix. There are two parameters that determine the pooling layers, (1) filtering  $F^l$  in the spatial domain, (2) the stride  $S^l$ . These layers create an output with a dimension of  $m_1^l \times m_2^l \times m_3^l$  while requiring input of size  $m_1^{(l-1)} \times m_2^{(l-1)} \times m_3^{(l-1)}$ . Equations (3) present maximum pooling approximation as described in the following equations.

$$\begin{aligned} m_1^{(l)} &= m_1^{(l-1)} \\ m_2^{(l)} &= \frac{m_2^{(l-1)} - F^{(l)}}{S^{(l)}} + 1 \\ m_3^{(l)} &= \frac{m_3^{(l-1)} - F^{(l)}}{S^{(l)}} + 1 \end{aligned} \quad (3)$$

The proceeding output layers are accepting only one-dimensional vectors due to the act of smoothing that has been done on the max-pooling layers. The following rule specifies the dimensions of the resultant vector.

$$n^{[i-1]} = n_h^{[i-1]} \times n_w^{[i-1]} \times n_c^{[i-1]} \quad (4)$$

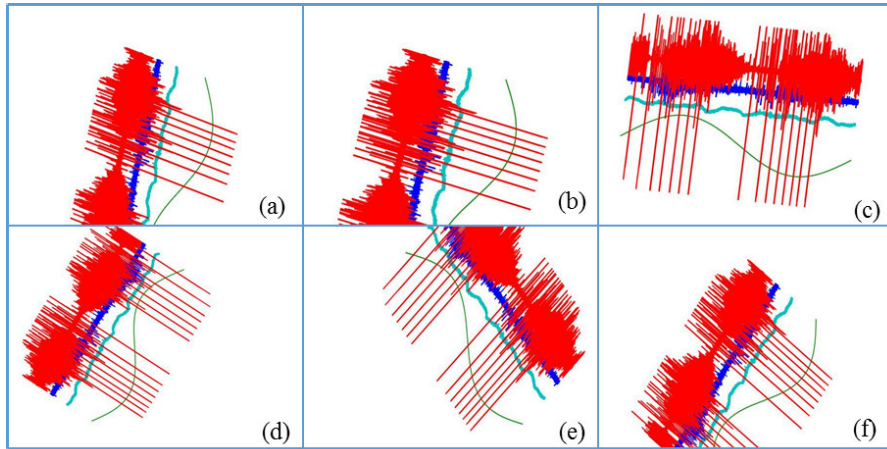


**FIGURE 2.** RGB images after applying data augmentation to PD type: (a) shear range of 0.2, (b) zoom range of 0.2, (c) rotation range of 90, (d) horizontal flip, (e) width shift range of 0.01, and (f) height shift range of 0.01.

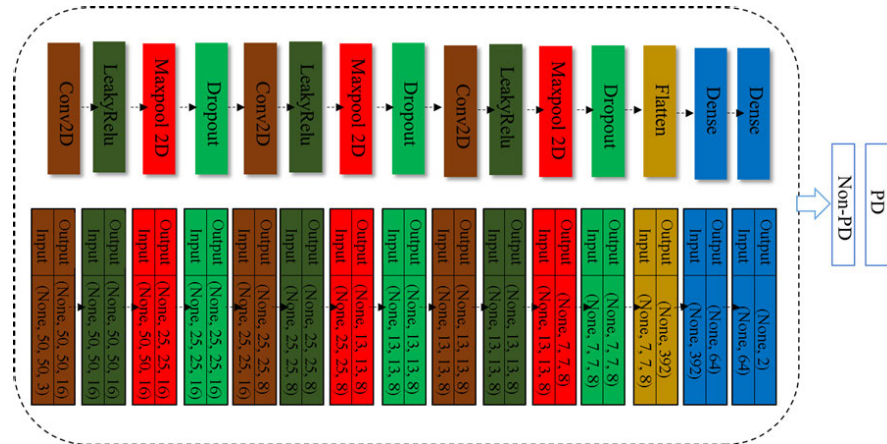


**FIGURE 3.** Proposed deep network architecture of CNN with RGB images.

where  $n_w$  is the width,  $n_h$  is  $i$ th layer height, and  $n_c$  is the channel count.

As a result of building relu function from a dense class, the last fully connected layers adapted the activation function (SoftMax) to serve as a detector. These layers have limited neurons and consider node ( $j$ th) out from layer ( $i$ th) to return a vector  $a^{[i]}$  from an input vector  $a^{[i-1]}$ . At the  $l$ th layer, the learned factors can be calculated as follows:

$$Z_j^{[l]} = \sum_{l=1}^{n_{i-1}} W_{j,l}^{[l]} a_l^{[i-1]} + b_j^{[l]} \rightarrow a_j^{[l]} = \psi^{[l]} \left( Z_j^{[l]} \right) \quad (5)$$

where  $W_{j,l}$ ,  $n_{l-1} * n_l$ ,  $b_j^{[l]}$ , and  $\psi^{[l]}$  stand for weights, weights' parameters, layer's bias, and activation function, respectively.

## 2) LONG SHORT-TERM MEMORY (LSTM)

The well-known advanced version of the recurrent neural network (RNN) is the LSTM [18]. As a default, LSTM can retain long-time info and is trained to acquire a knowledge of dependent long-term memory. The duplicating module is structured as a chain even if its architecture is distinct [19]. The LSTM contains four interacting layers whereas each layer has its

own means of communication. Cells (cell and hidden states) are the units of memory that make up an LSTM network in its most basic form. The hidden state is intended to encode a form of characterization of the data from the previous time step, whereas the cell state is intended to encode an aggregate of data from all previously processed time-steps. These states are both transmitted to the subsequent cell. The primary chain of data flow is the cell state, which enables the data to move ahead mostly unchanged. However, there may be some linear modifications. Data can be added to or removed from the cell state using sigmoid gates. An equivalent of a gate is a layer or sequence of matrix operations that have various discrete weights. These gates are designed to control the data-saving procedure. The operations of memorizing data are organized by these gates.

LSTM-based PD recognition model was constructed on RGB and gray images, and its components are shown in Fig. 4, where the first layer was the input data for RGB (None, 2500, 3) or gray-scale images (None, 2500, 1). In this work, the LSTM model's structure for both RGB and grayscale images is identical except for a unique difference observed in the first layer. Another layer in this model called dropout

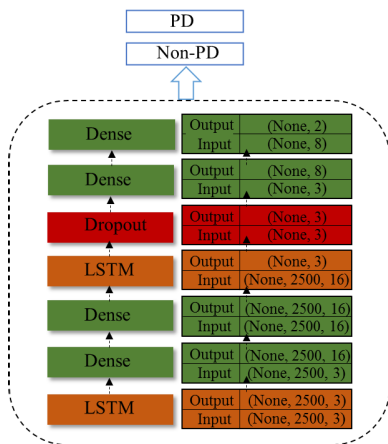


FIGURE 4. A deep network LSTM architecture with RGB images.

arose to decrease over-fitting DL models [20]. The term “dense layer,” also known as a “fully connected layer,” describes a layer whose internal neurons are coupled to every neuron in the proceeding layer. A matrix-vector multiplication is utilized to update a vector’s dimensions. Backpropagation can aid in the training and updating of matrix values. Since there are more than two class labels, SoftMax was utilized as an activation function to predict a multinomial probability distribution. The category with the highest likelihood will be used by the model to create a precise forecast.

**B. HYBRID DEEP NETWORK ARCHITECTURE**

This study analyzed different forms of space color images (RGB and gray) when training CNN and LSTM models. The hybrid deep network’s architecture combined CNN and LSTM models. F1, features generated by CNN algorithm, and F2, features produced by an LSTM-based model, were the two features that were recovered from these sources. With a high level of precision, the hybrid model’s properties offered a reliable categorization of PD.

**C. CLASSIFICATION PERFORMANCE EVALUATION**

Overall accuracy Acc, precision Pr, recall Re, intersection over union IoU, and F-measure (Fm) measurements were used to quantitatively evaluate the performance of the suggested deep networks. These measures are detailed in the following equations.

$$\begin{aligned}
 Acc &= \frac{\sum TP + \sum TN}{\sum TP + \sum TN + \sum FP + \sum FN} \times 100 \\
 IoU &= \frac{TP}{FP + TP + FN} \times 100 \\
 Pr &= \frac{\sum TP}{\sum TP + \sum FP} \times 100 \\
 Re &= \frac{\sum TP}{\sum TP + \sum FN} \times 100 \\
 Fm &= 2 * \left( \frac{Pr * Re}{Pr + Re} \right) \times 100
 \end{aligned}
 \tag{6}$$

where TP is true positive, TN is true negative, FP is false positive, and FN is false negative.

**IV. RESULTS AND DISCUSSIONS**

**A. ASSESSMENT OF THE CNN-BASED MODEL**

The proposed model for monitoring the partial discharge images was based on different properties retrieved from gray and RGB images. Throughout the training process, features were extracted and normalized before they have been used as input into the deep learning model. The model identified the patterns associated with partial discharge in the data and leveraged this understanding to make predictions about future occurrences. As shown in Table 1, the CNN deep network outcomes (accuracy and losses) were evaluated with training and validation datasets. As well, the classification performance was examined. The CNN-RGB technique exhibited superior performance compared to the CNN-gray algorithm, as indicated by the accuracy metrics. The proposed method’s performance achieves a recall = 0.961, precision = 0.956, over union = 0.925, and F-measure = 0.955. The model shows validation of an accuracy=0.961 and a model-loss (M-loss) =0.093.

**B. ASSESSMENT OF THE LSTM-BASED MODEL**

The LSTM model was executed with gray and RGB images for evaluating the classification performance. Table 2 shows the training model, the validation model, and the performance model for RGB and Gray images. With respect to the LSTM model, RGB color space images had better partial discharge definition with recall = 0.947, precision = 0.896, over union = 0.899 and F-measure = 0.921. The model validation shows an accuracy of 0.947 and an M-loss of 0.208. Apparently, the CNN model demonstrated a higher accuracy (96.1%) compared to the LSTM model (94.7%). In contrast to LSTM model (94.7%), the CNN model demonstrated a higher accuracy (96.1%).

**C. EVALUATION OF THE HYBRID DEEP NETWORK**

Various types of images including RGB and grayscale were executed as the main source input for the LSTM and CNN model. Likewise, image data augmentation has been performed to evaluate the studied methodologies. The classification model of CNN-LSTM was evaluated as explained in Table 3, and performance metrics (Pr, Re, Fm, and IoU) were used to validate the strength of the model in monitoring partial discharge. The CNN-LSTM model outputs based on the augmentation technique accomplish great precision using gray and RGB images. The results in Table 3 approved that the CNN-LSTM-RGB and CNN-LSTM-gray models with augmented versions were high-quality models for partial discharge identification as opposed to hybrid deep models with non-augmented versions. The model achieves a validation accuracy, of 0.999, and a loss model, of 0.004.

TABLE 1. Results of CNN deep network using partial discharge images.

Model	Image	Training			Validation		Performance			
		Acc	Ls	Tt	Acc	Ls	Pr	Re	Fm	IoU
CNN	Gary	0.963	0.103	2.648	0.950	0.132	0.943	0.949	0.943	0.904
	RGB	0.966	0.092	3.414	0.961	0.093	0.956	0.961	0.955	0.925

TABLE 2. Results of LSTM deep network using partial discharge images.

Model	Image	Training			Validation		Performance			
		Acc	Ls	Tt	Acc	Ls	Pr	Re	Fm	IoU
LSTM	Gary	0.942	0.221	89.417	0.934	0.244	0.872	0.934	0.902	0.876
	RGB	0.937	0.236	74.759	0.947	0.208	0.896	0.947	0.921	0.899

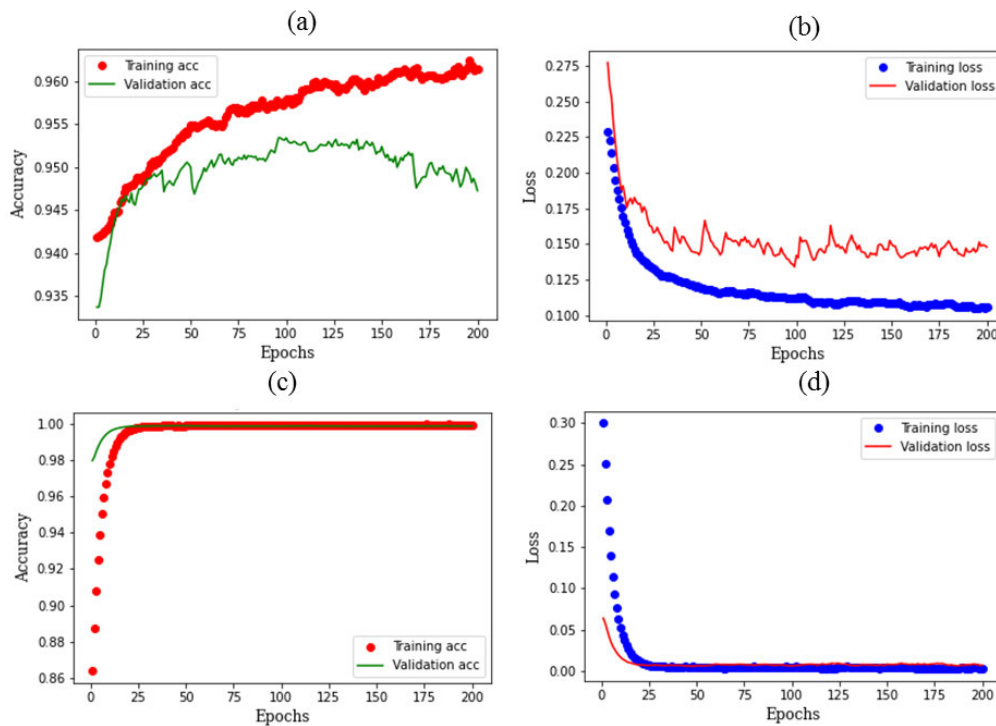


FIGURE 5. Evaluation metrics of partial discharge detection model of CNN-LSTM based on gray images (a, b) non-augmented version, and (c, d) augmented version.

TABLE 3. Results of hybrid deep network using partial discharge images.

Model	Image	Aug (PD)	Training			Validation		Performance			
			Acc	Ls	Tt	Acc	Ls	Pr	Re	Fm	IoU
CNN-LSTM	Gary	No	0.969	0.089	75.734	0.953	0.123	0.949	0.953	0.943	0.910
		Yes	1.0	0.0003	104.382	0.999	0.004	0.999	0.999	0.999	0.998
	RGB	No	0.966	0.095	73.420	0.961	0.096	0.956	0.960	0.957	0.923
		Yes	0.999	0.002	105.751	0.999	0.004	0.999	0.999	0.999	0.998

D. DEEP NEURAL NETWORK LEARNING CURVE

The learning curve of the detection model was improved by selecting the upper-most parameters, adapting the selection

features using the deep learning model, and investigating the architectural components of the deep network. While these operations were being carried out, novel hybrid deep

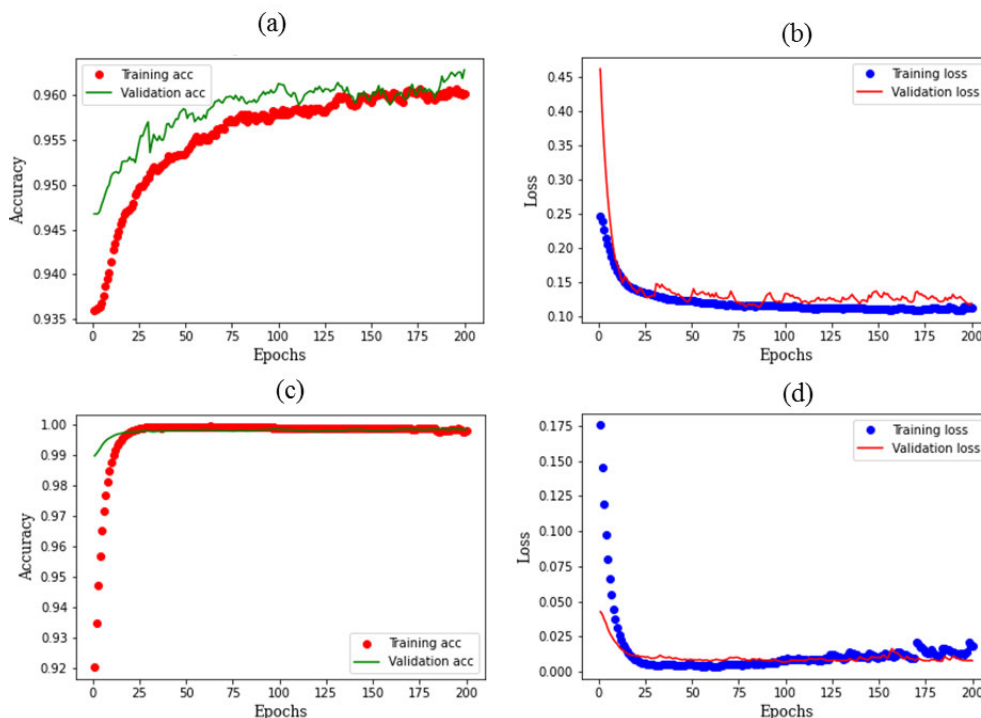


**FIGURE 6.** Evaluation metrics of partial discharge detection model of CNN-LSTM based on RGB images: (a, b) non-augmented version, and (c, d) augmented version.

networks were established. The CNN-LSTM behavior using higher variations recovered from gray and RGB images during the training and validation set is explained in Fig. 5, 6. The learning curves of the CNN-LSTM-gray model attained a validation accuracy of 95.3% ( $L_s=0.123$ ) and 99.9% ( $L_s=0.004$ ), for non-augmented (Fig. 5 (a-b)) and augmented (Fig. 5 (c-d)) versions, respectively. Otherwise, the validation accuracies of the CNN-LSTM-RGB model with non-augmented (Fig.6 (a-b)) and augmented (Fig. 5 (c-d)) versions were 96.1% ( $L_s=0.096$ ) and 99.9% ( $L_s=0.004$ ), respectively. As the number of epochs grows, the accuracy of validation and training gradually improves until the learning graph indicates a high-quality model. Simultaneously, the loss of the models reduces steadily. It is observed that validation accuracy is typically less than training accuracy. In comparison to other models, the features extracted from RGB or gray-scale using CNN-LSTM and the data augmentation approach performed well in recognizing the PD. It had a 99.9% classification accuracy for Pr, Re, and Fm, with a 99.8% of IoU, and excellent learning curve performance outcomes.

**E. CLASSIFICATION MODELS EVALUATIONS**

The proposed CNN-LSTM-gray and LSTM-LSTM-RGB models for PD-type classification have matrix confusion during the phase of validation as shown in Fig. 7. It was realized that approximately 114 and 104 images were misclassified by the models which did not use the data augmentation as presented in Fig. 7 (a-c). Although, the models that adapted data augmentation correctly classified the images as

presented in Fig. 7 (b-d). Since the true positive and true negative have consistent values and there are no all falling positive or negative, the proposed CNN-LSTM model that was developed with a data augmentation strategy accomplished better results compared to other network models. As a result, the suggested approach can efficiently classify partial discharge. It outperforms prior studies in terms of performance, making it a viable tool for representing PD patterns. The outcomes achieved greater accuracy than those of Kim and Kim K-I [21], who explained that the suggested CNN transfer-learning models, which used a little amount of actual PD data acquired from an online PD detection system, outperformed benchmark models like CNN and SVM in terms of PD detection accuracy (97.4). Additionally, the developed model outperformed [22], the light-scale CNN model that was used in GIS for PD recognition. In this experiment, artificial defects were produced, and PD faults were acquired using a UHF sensor. Two convolution layers, two max-pooling layers, and two fully linked layers were included in the light-scale model. The model had an overall accuracy of 98.13%. The overall performance of the proposed hybrid network shows precise results, especially when compared with [23] which examined the ensemble technique and LSTM deep learning for PD classification. The ensemble bagged decision trees and LSTM deep learning achieved accuracies of 95.5% and 98.3%, respectively. The upgraded models achieved great classification performance while incurring smaller losses. Electrical engineers can rely on our methodology, which demands frequent, fast, easy, and non-destructive detection of partial discharge at high voltage.

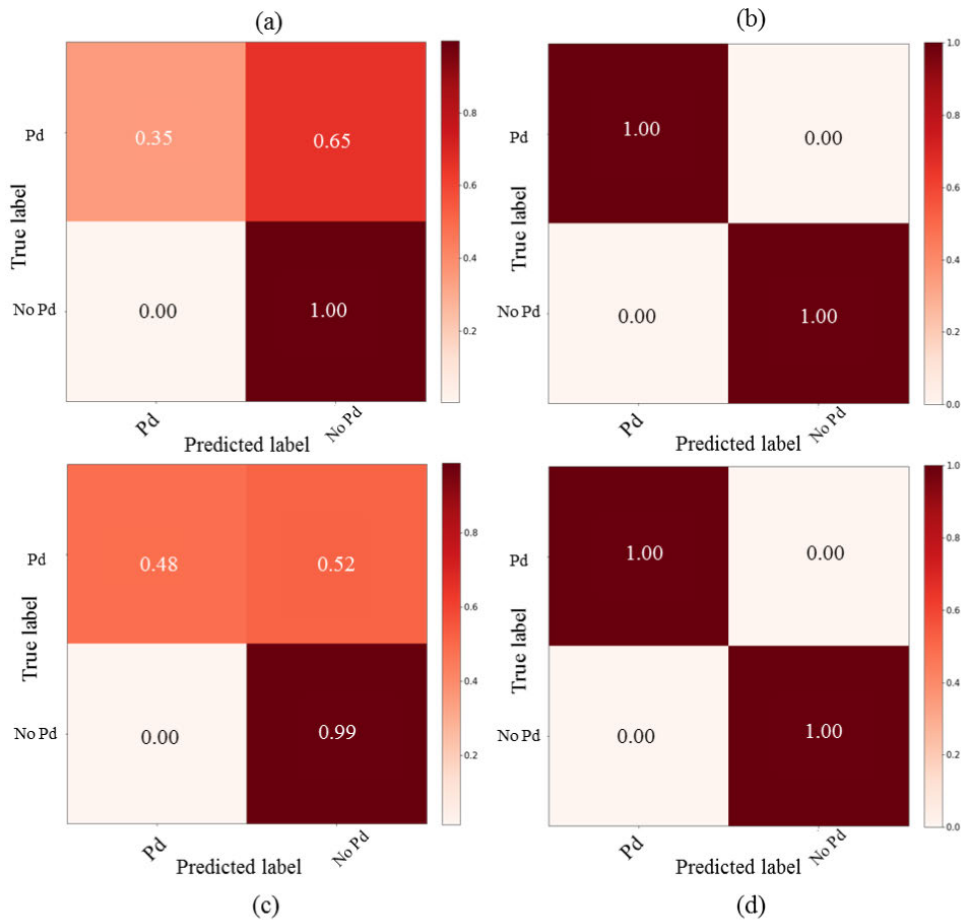


**FIGURE 7.** Confusion matrix of proposed CNN-LSTM models for detecting partial discharge in grayscale and RGB images via: (a, c) non-augmented version and (b, d) augmented version.

## V. CONCLUSION

It is difficult to distinguish partial discharge (PD) caused by numerous insulation flaws in cables with high voltage. Even for the most seasoned professionals, some PD signals might be challenging to detect since they have remarkably similar qualities. To tackle the difficulty, a robust hybrid approach for identifying PD patterns has been developed by combining LSTM and CNN. The proposed framework has been promoted for robust detection of PD type through some actions including characteristics of features selected through hybrid deep network training, choosing the most significant hyper-parameters, and optimum components of the deep network architecture. The planned implementation has been compared to a single deep network for CNN and LSTM. A high-quality model was then found by analyzing the performance outcomes. Analysis outcomes elucidated that the supreme combinations for PD pattern identification between deep networks and the data augmentation methods according to the highest performance were CNN-LSTM-RGB and CNN-LSTM-gray. Their corresponding outputs for precision (99.9%), recall (99.9%), F-measure (99.9%), and intersection over union (99.8%) were identical. These models demonstrated promising outcomes with high accuracy and were

employed to define the pattern of PD. The accurate recognition of PD through hybrid deep-learning network models can significantly impact various sectors. By recognizing PD accurately, deep network models can predict faults in power systems, triggering preventive maintenance and preventing potential catastrophic failures. This can result in significant cost savings and improved system reliability. Early detection and rectification of PD can potentially prolong the life of the electrical equipment, reducing replacement costs and downtime. Improved PD recognition can enhance the safety of power systems by identifying potential faults before they lead to accidents or power outages. In the context of smart grids, accurate PD recognition can contribute to effective asset management and maintenance scheduling, leading to more efficient and reliable power distribution. Finally, this study has introduced a tool that offers a swift and simple approach, potentially enabling power system experts to make superior real-time decisions. Finally, this tool is a quick and easy strategy that may help power systems professionals make excellent real-time judgments. In the future, we advocate expanding the usage of the superlative model to additional insulating challenges in high-voltage cables in order to accomplish power system stability.



## REFERENCES

- [1] J. Li, X. Han, Z. Liu, and X. Yao, "A novel GIS partial discharge detection sensor with integrated optical and UHF methods," *IEEE Trans. Power Del.*, vol. 33, no. 4, pp. 2047–2049, Aug. 2018.
- [2] T. Shao, F. Kong, H. Lin, Y. Ma, Q. Xie, and C. Zhang, "Correlation between surface charge and DC surface flashover of plasma treated epoxy resin," *IEEE Trans. Dielectr. Electr. Insul.*, vol. 25, no. 4, pp. 1267–1274, Aug. 2018.
- [3] A. Hirata, S. Nakata, and Z.-I. Kawasaki, "Toward automatic classification of partial discharge sources with neural networks," *IEEE Trans. Power Del.*, vol. 21, no. 1, pp. 526–527, Jan. 2006.
- [4] L. Zhu, F. Hou, S. Ji, H. Rehman, and X. Wu, "Primary differential pulse method for partial-discharge detection of oil-immersed inverted current transformers," *IEEE Trans. Power Del.*, vol. 33, no. 3, pp. 1492–1494, Jun. 2018.
- [5] J. Tang, F. Liu, X. Zhang, X. Liang, and Q. Fan, "Partial discharge recognition based on SF6 decomposition products and support vector machine," *IET Sci., Meas. Technol.*, vol. 6, no. 4, pp. 198–204, 2012.
- [6] L. Li, J. Tang, and Y. Liu, "Partial discharge recognition in gas insulated switchgear based on multi-information fusion," *IEEE Trans. Dielectr. Electr. Insul.*, vol. 22, no. 2, pp. 1080–1087, Apr. 2015.
- [7] L. Hao and P. Lewin, "Partial discharge source discrimination using a support vector machine," *IEEE Trans. Dielectr. Electr. Insul.*, vol. 17, no. 1, pp. 189–197, Feb. 2010.
- [8] F. Liu, C. Shen, G. Lin, and I. Reid, "Learning depth from single monocular images using deep convolutional neural fields," *IEEE Trans. Pattern Anal. Mach. Intell.*, vol. 38, no. 10, pp. 2024–2039, Oct. 2016.
- [9] S. Bae and K. Yoon, "Confidence-based data association and discriminative deep appearance learning for robust online multi-object tracking," *IEEE Trans. Pattern Anal. Mach. Intell.*, vol. 40, no. 3, pp. 595–610, Mar. 2018.
- [10] G. Li, X. Wang, X. Li, A. Yang, and M. Rong, "Partial discharge recognition with a multi-resolution convolutional neural network," *Sensors*, vol. 18, no. 10, p. 3512, Oct. 2018.
- [11] T. Liu, J. Yan, Y. Wang, Y. Xu, and Y. Zhao, "GIS partial discharge pattern recognition based on a novel convolutional neural networks and long short-term memory," *Entropy*, vol. 23, no. 6, p. 774, Jun. 2021.
- [12] A. Buslaev, V. I. Iglovikov, E. Khvedchenya, A. Parinov, M. Druzhinin, and A. A. Kalinin, "Albumentations: Fast and flexible image augmentations," *Information*, vol. 11, no. 2, p. 125, Feb. 2020.
- [13] W. Yijiang, L. Chen, W. Ganjun, P. Xiaosheng, L. Taiwei, and Z. Yunzheng, "Partial discharge data augmentation of high voltage cables based on the variable noise superposition and generative adversarial network," in *Proc. Int. Conf. Power Syst. Technol. (POWERCON)*, Nov. 2018, pp. 3855–3859.
- [14] X. Peng, F. Yang, G. Wang, Y. Wu, L. Li, Z. Li, A. A. Bhatti, C. Zhou, D. M. Hepburn, A. J. Reid, M. D. Judd, and W. H. Siew, "A convolutional neural network-based deep learning methodology for recognition of partial discharge patterns from high-voltage cables," *IEEE Trans. Power Del.*, vol. 34, no. 4, pp. 1460–1469, Aug. 2019.
- [15] E. W. Nery and L. T. Kubota, "Sensing approaches on paper-based devices: A review," *Anal. Bioanal. Chem.*, vol. 405, no. 24, pp. 7573–7595, Sep. 2013.
- [16] X. Zhou, X. Wu, P. Ding, X. Li, N. He, G. Zhang, and X. Zhang, "Research on transformer partial discharge UHF pattern recognition based on CNN-lstm," *Energies*, vol. 13, no. 1, p. 61, Dec. 2019.
- [17] J. R. Ubbens and I. Stavness, "Deep plant phenomics: A deep learning platform for complex plant phenotyping tasks," *Frontiers Plant Sci.*, vol. 8, p. 1190, Jul. 2017.
- [18] S. Hochreiter and J. Schmidhuber, "Long short-term memory," *Neural Comput.*, vol. 9, no. 8, pp. 1735–1780, 1997.
- [19] C. Olah, "Understanding LSTM networks," in *Proc. GitHub Blog*, Aug. 2015. [Online]. Available: <http://colah.github.io/posts/2015-08-Understanding-LSTMs/>
- [20] N. Srivastava, G. Hinton, A. Krizhevsky, I. Sutskever, and R. Salakhutdinov, "Dropout: A simple way to prevent neural networks from overfitting," *J. Mach. Learn. Res.*, vol. 15, no. 1, pp. 1929–1958, Jan. 2014.
- [21] J. Kim and K.-I. Kim, "Partial discharge online detection for long-term operational sustainability of on-site low voltage distribution network using CNN transfer learning," *Sustainability*, vol. 13, no. 9, p. 4692, Apr. 2021.
- [22] Y. Wang, J. Yan, Z. Yang, T. Liu, Y. Zhao, and J. Li, "Partial discharge pattern recognition of gas-insulated switchgear via a light-scale convolutional neural network," *Energies*, vol. 12, no. 24, p. 4674, Dec. 2019.
- [23] E. Balouji, T. Hammarström, and T. McKelvey, "Partial discharge classification in power electronics applications using machine learning," in *Proc. IEEE Global Conf. Signal Inf. Process. (GlobalSIP)*, Nov. 2019, pp. 1–5.



**OBABD ALDOSARI** (Member, IEEE) received the B.Sc. and M.Sc. degrees in electrical engineering from Western Michigan University, Kalamazoo, MI, USA, in 2013 and 2014, respectively, and the Ph.D. degree in electrical engineering from the University of Arkansas, Fayetteville, AR, USA, in 2020. He is currently an Assistance Professor with the Electrical Department, College of Engineering at Wadi Ad-Dawasir, Prince Sattam Bin Abdulaziz University, Wadi Ad-Dawasir, Saudi Arabia. His current research interests include power electronics, renewable energy systems, artificial neural network (ANN) and its applications in power electronics, high-frequency transformer design, and electrical vehicles. He is a member of the Honor Societies Eta Kappa Nu and Tau Beta Pi.



**MOHAMMED A. ALDOWSARI** (Member, IEEE) received the B.Sc. and M.Sc. degrees in electrical engineering from Prince Sattam Bin Abdulaziz University and King Khalid University, respectively. He is currently a senior engineer executing power system-related studies. Aldowsari is a registered Professional Engineer with the Engineering Council of Saudi Arabia. His research interests include the optimization of distributed energy resources DERs, hybrid optimization technique, renewable energy system, and artificial intelligence applications in power systems where he obtained a professional certificate from IBM in Artificial Intelligence Engineering.



**SALEM BATIYAH** (Member, IEEE) received the Ph.D. degree from the Department of Electrical and Computer Engineering, Mississippi State University, in 2020. He is currently an Assistant Professor with the Electrical and Electronics Engineering Technology Department, Yanbu Industrial College, Yanbu Industrial, Saudi Arabia. His current research interests include renewable energy integration, control of power electronic converters, model predictive control, and power management systems.



**N. KANAGARAJ** (Member, IEEE) received the B.E. degree from Bharathiar University, Tamil Nadu, India, and the M.Tech. and Ph.D. degrees from the National Institute of Technology (NIT), Tiruchirappalli, Tamil Nadu. He is currently a Professor with the Department of Electrical Engineering, College of Engineering at Wadi Al-Dawasir, Prince Sattam Bin Abdulaziz University, Saudi Arabia. His research interests include fuzzy logic control, system identification, maximum power point tracking, and renewable energy systems.

...